Electronic Supplementary Material (ESI) for Journal of Materials Chemistry A.

Supporting Information

An amorphous/nanocrystalline Ni_xP/Ni heterojunction for electrooxidation of hydrazine

Jia-Fu Liu, He Wen, Zeng-Yao Zhang and Ping Wang*

School of Materials Science and Engineering, South China University of Technology, Guangzhou 510641, P. R. China

*Corresponding Author.

E-mail: mspwang@scut.edu.cn (P. Wang)

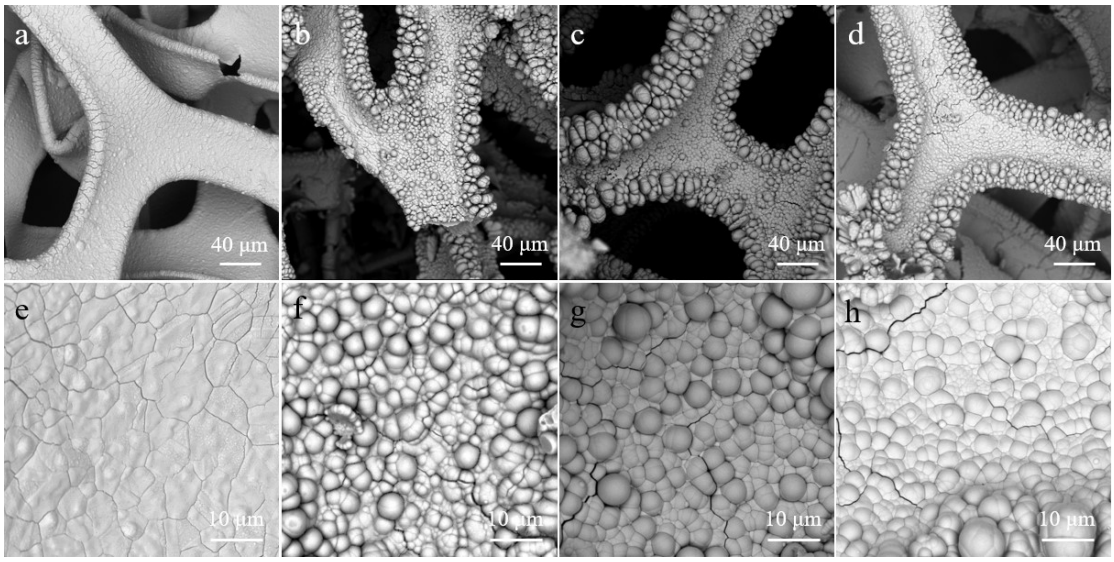

Figure S1. SEM images at different magnifications of the *a*-Ni_xP/Ni/NF catalysts prepared by electrodeposition for a duration of (a, e) 15 min, (b, f) 30 min, (c, g) 60 min, (d, h) 90 min.

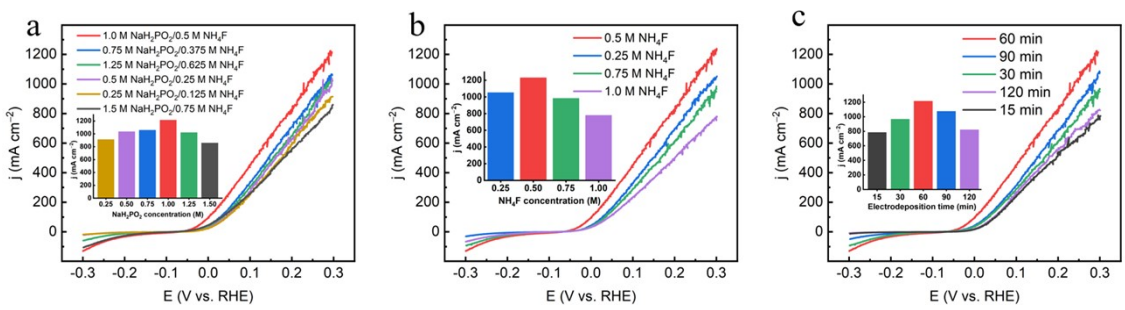

Figure S2. (a) LSV curves of the samples that were electrodeposited in the electrolyte of different concentrations of NaH_2PO_2 and NH_4F. The inset shows the current density dependence on the NaH_2PO_2 concentration. The current density values were extracted from (a) at 0.3 V vs. RHE. (b) LSV curves of the samples that were electrodeposited in the electrolyte of different concentrations of NH_4F while keeping the NaH_2PO_2 concentration at 1 M. The inset shows the current density dependence on the NH_4F concentration. (c) LSV curves of the samples that were electrodeposited in an electrolyte of 1.0 M NaH_2PO_2/0.5 M NH_4F for different durations. The inset shows the current density dependence on the electrodeposition duration. All electrochemical tests were carried out in an electrolyte containing 0.5 M $N_2H_4{\cdot}H_2O$ and 1 M NaOH.

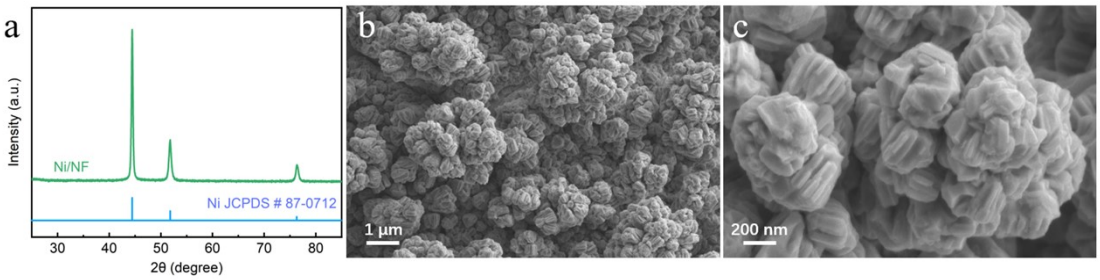

Figure S3. (a) XRD pattern and (b, c) SEM images of the Ni/NF catalyst prepared by electrodeposition method using an electrolyte without P source. In preparation of the samples for XRD analysis, we used Cu foil to replace Ni foam at cathode side. The thus-prepared samples were then scraped off from Cu foil.

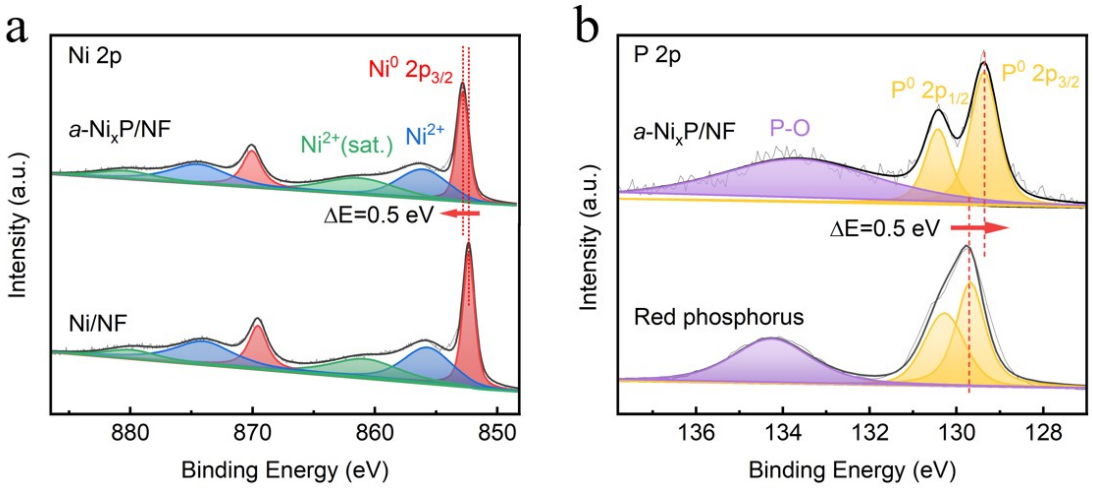

Figure S4. XPS spectra of the *a*-Ni_xP/NF catalyst and Ni/NF, red phosphorus reference samples in the Ni 2p and P 2p regions.

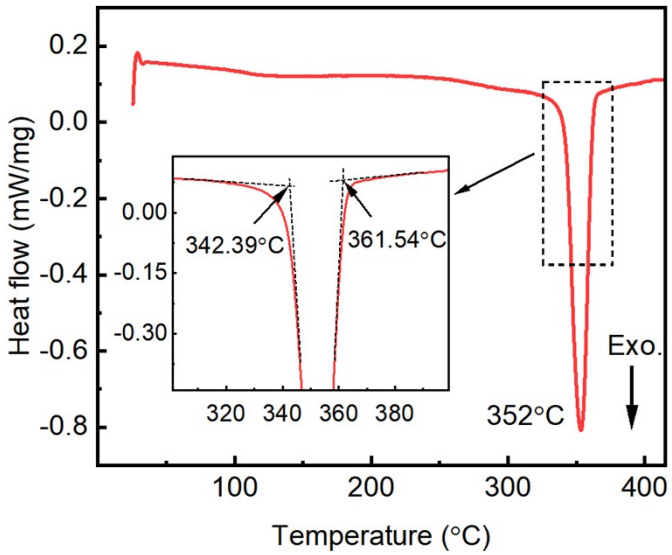

Figure S5. DSC curve of the *a*-Ni_xP/Ni sample. The inset shows an enlarged view of the section of interest.

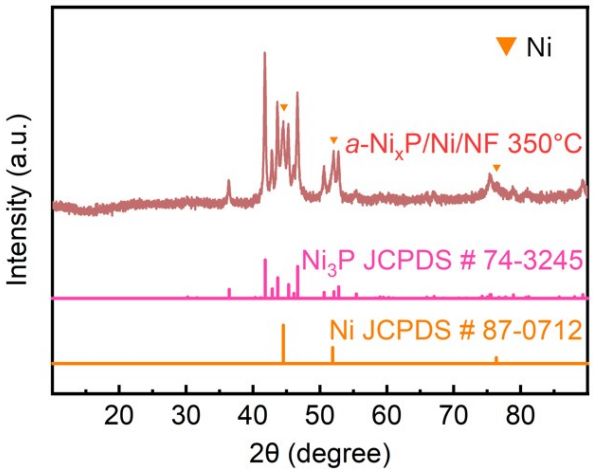

Figure S6. XRD pattern of the calcined catalyst at 350 °C under Ar atmosphere for 1 h.

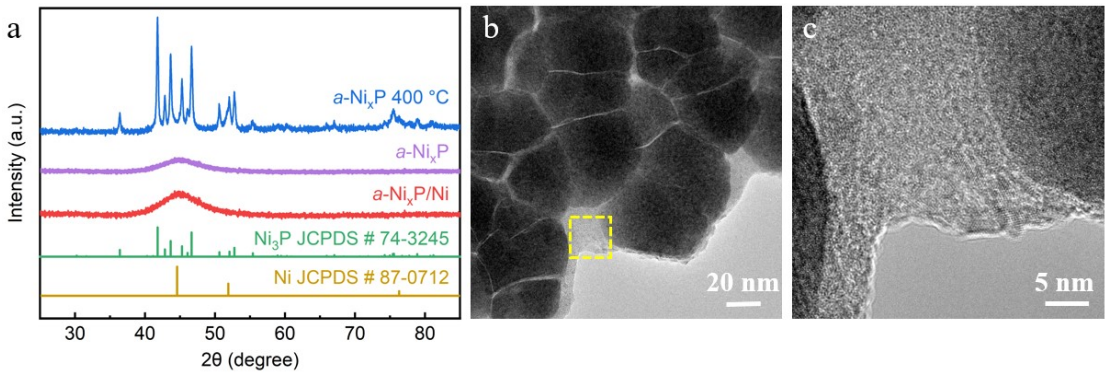

Figure S7. (a) XRD patterns of *a*-Ni$_x$P/Ni, *a*-Ni$_x$P and the post-calcined *a*-Ni$_x$P at 400 °C under Ar atmosphere for 1 h. (b) TEM image and (c) HRTEM image of *a*-Ni$_x$P.

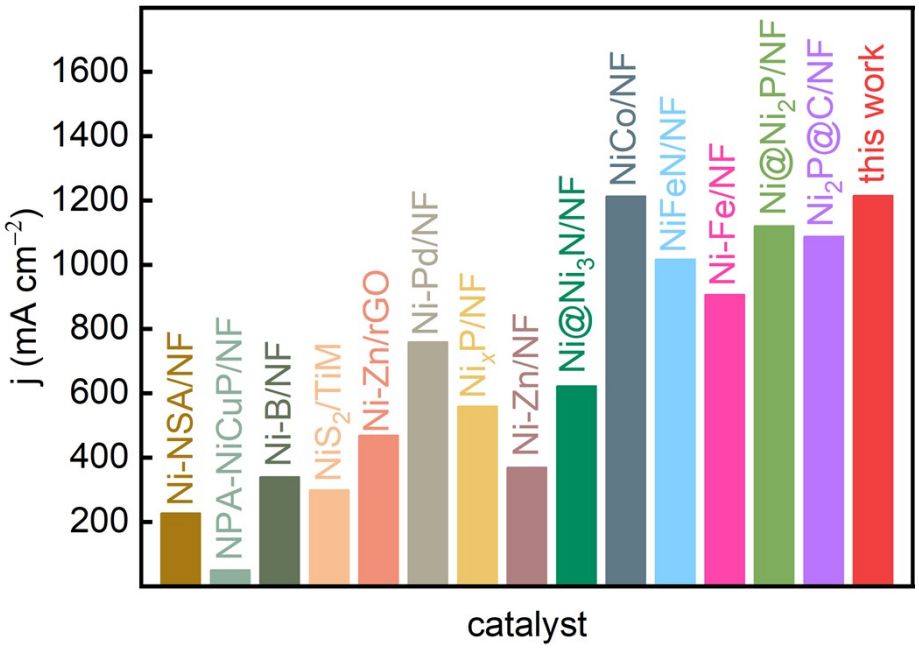

Figure S8. A comparison of catalytic activities of representative HzOR electrocatalysts. The measurement conditions of the catalysts can be found in Table S2.

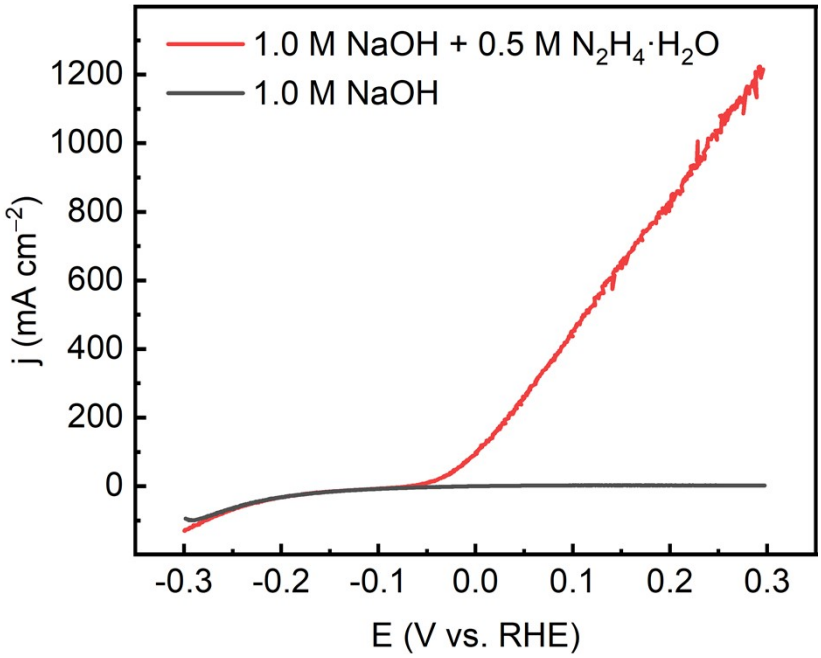

Figure S9. A comparison of the LSV curves of the *a*-Ni_xP/Ni/NF catalyst in an electrolyte with and without $N_2H_4 \cdot H_2O$, respectively.

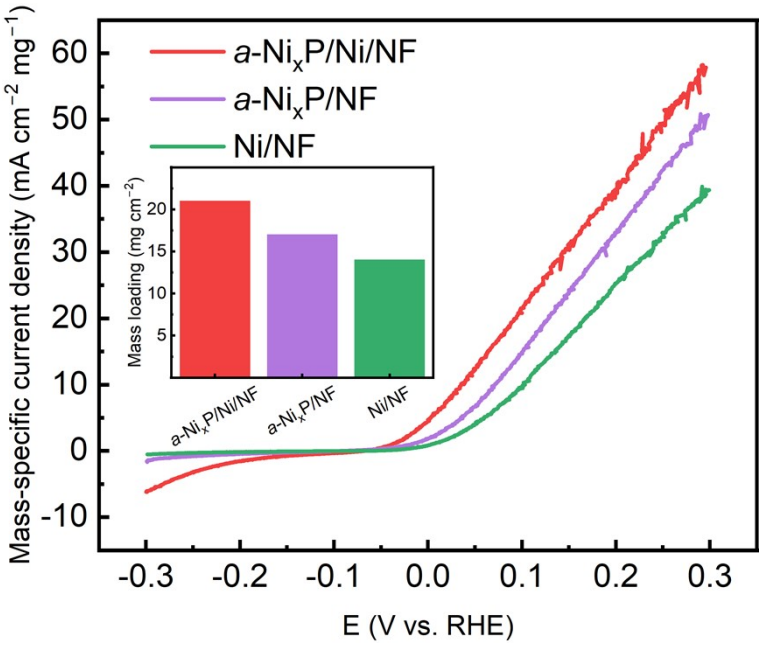

Figure S10. Mass-specific current densities and mass loadings (inset) of *a*-Ni_xP/Ni/NF, *a*-Ni_xP/NF, and Ni/NF catalysts.

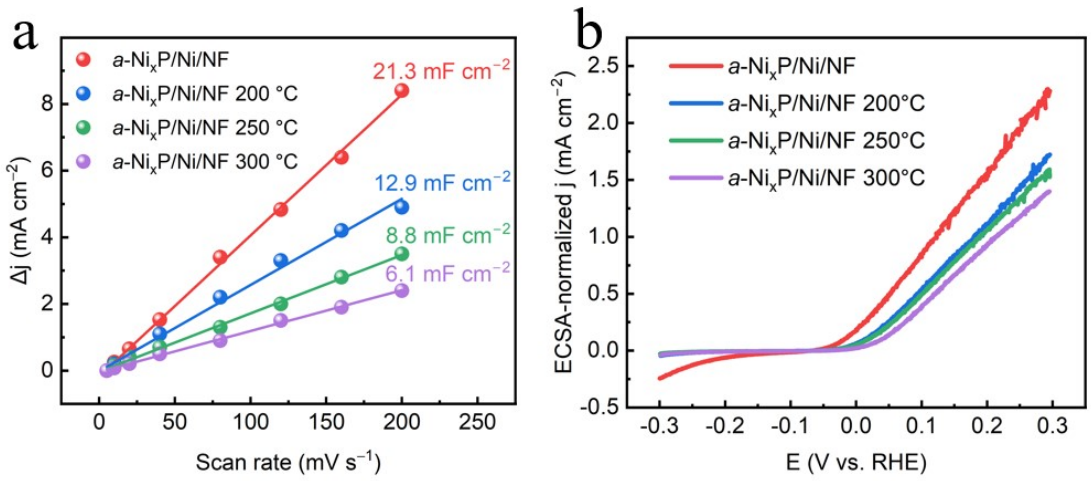

Figure S11. (a) Plots of capacitive current density as a function of scan rate at OCP and (b) the ECSA-normalized activities of *a*-Ni$_x$P/Ni/NF and its crystalline counterparts.

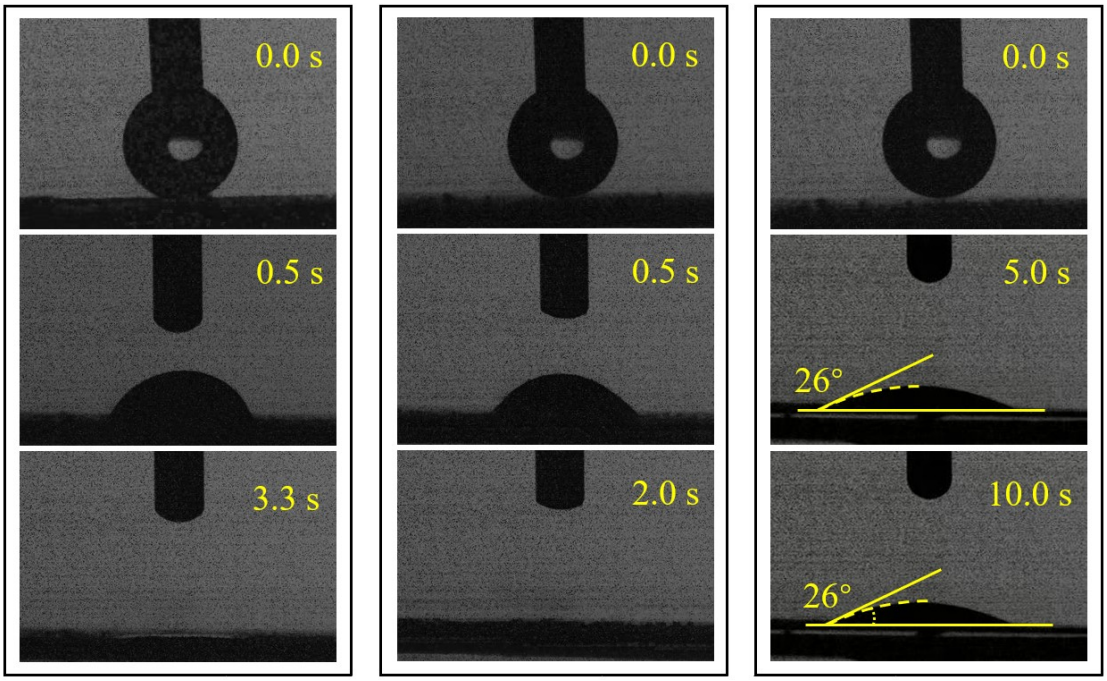

Figure S12. Contact-angle measurement results of (left) *a*-Ni_xP/Ni/NF, (middle) *a*-Ni_xP/NF and (right) Ni/NF.

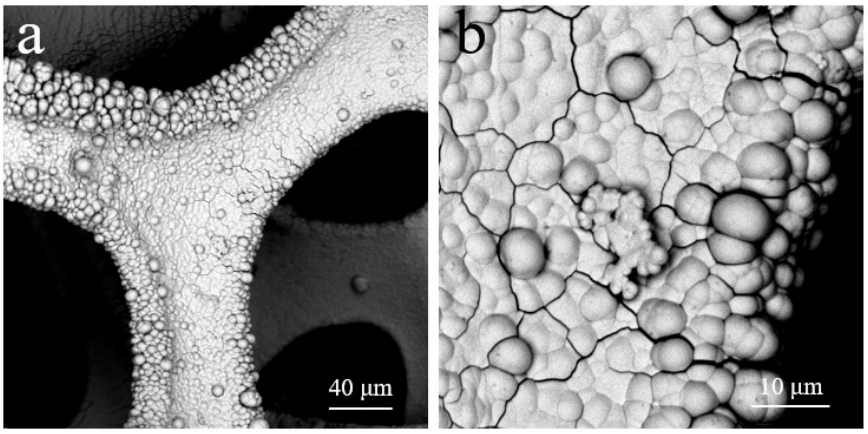

Figure S13. FE-SEM images of the *a*-Ni_xP/NF catalyst at different magnifications.

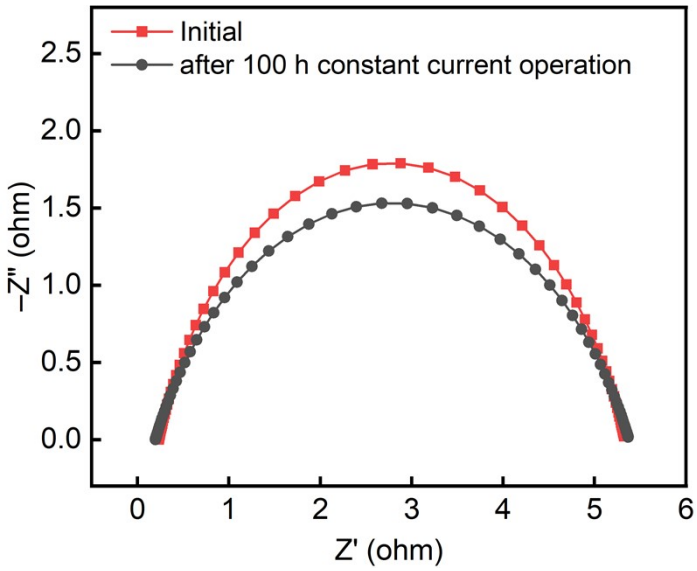

Figure S14. EIS Nyquist plots of the *α*-Ni_xP/Ni/NF catalyst before and after 100 hours of constant current operation.

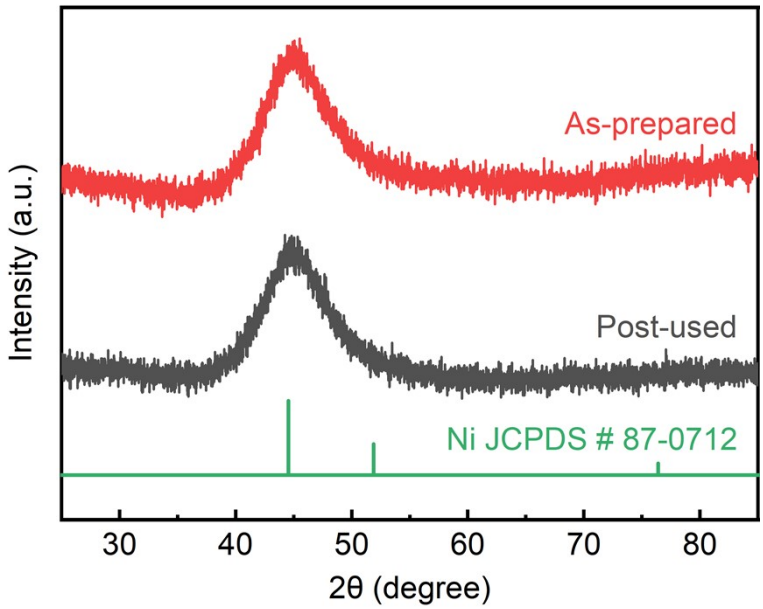

Figure S15. A comparison of the XRD patterns of the as-prepared and post-used *a*-Ni_xP/Ni catalysts.

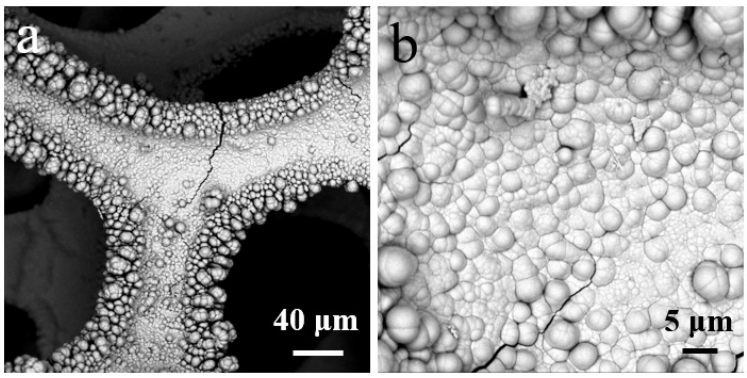

Figure S16. FE-SEM images of *a*-Ni_xP/Ni/NF after 100 hours of operation.

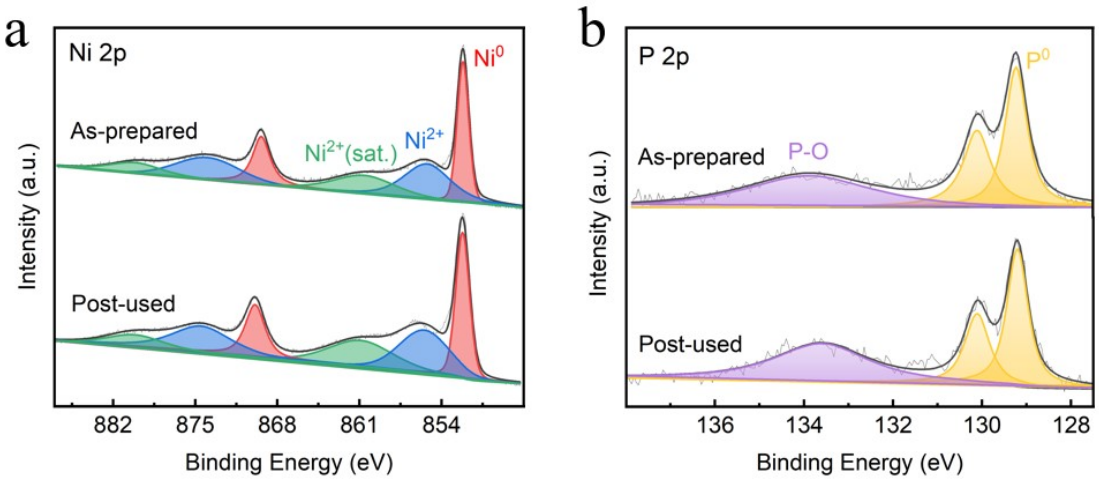

Figure S17. XPS spectra of the as-prepared and post-used *a*-Ni_xP/Ni/NF catalysts in the Ni 2p and P 2p regions.

Table S1. Chemical composition of the samples that were electrodeposited at room temperature using the electrolyte of different concentrations of NaH_2PO_2 and NH_4F.

Sample	Electrolyte (M)		Ni (at%)	P (at%)
	NaH_2PO_2	NH_4F		
α-Ni_xP/Ni-1#	0.250	0.125	85.85	14.15
α-Ni_xP/Ni-2#	0.500	0.250	83.69	16.31
α-Ni_xP/Ni-3#	0.750	0.375	80.61	19.39
α-Ni_xP/Ni-4#	1.000	0.500	78.92	21.08
α-Ni_xP/Ni-5#	1.250	0.625	78.55	21.45
α-Ni_xP/Ni-6#	1.500	0.750	78.74	21.26
α-Ni_xP/Ni-7#	1.000	0.250	81.08	18.92
α-Ni_xP/Ni-8#	1.000	0.750	78.73	21.27
α-Ni_xP/Ni-9#	1.000	1.000	78.48	21.52
α-Ni_xP[a]	1.000	1.000	74.97	25.03

[a] Electrodeposited at 60 °C

Table S2. A comparison of the electrocatalytic performance of representative self-supported HzOR catalysts

Catalyst	Electrolyte (M)		Electrocatalytic performance			Reference
	N_2H_4	OH^-	*E* (V vs. RHE)	*j* (mA cm^{-2})	FE (%)	
Ni-NSA	0.5	3.0	0.25	227.6	/	[1]
NPA-NiCuP	0.005	1.0	0.35	51.4	/	[2]
Ni-B/NF	0.1	1.0	0.30	340	100	[3]
NiS_2/TiM	0.5	1.0	0.22	300	100	[4]
Ni-Zn/rGO	0.1	1.0	0.30	469	100	[5]
Ni-Pd/NF	0.1	1.0	0.60	760	100	[6]
Ni_xP/NF	0.1	1.0	0.30	580	100	[7]
Ni-Zn/NF	0.1	1.0	0.30	370	100	[8]
Ni@Ni_3N/NF	0.5	1.0	0.30	623	100	[9]
Ni-Co/NF	0.5	1.0	0.30	1213	100	[10]
NiFeN/NF	0.5	1.0	0.30	1017	100	[11]
Ni-Fe/NF	0.5	1.0	0.30	907	100	[12]
Ni@Ni_2P/NF	0.5	1.0	0.30	1120	100	[13]
Ni_2P@C/NF	0.5	1.0	0.30	1088	100	[14]
α-Ni_xP/Ni/NF	0.5	1.0	0.30	1215	100	This work

[a] All potentials were obtained with respect to the RHE at pH=14.

[b] FE denotes Faradaic efficiency.

Table S3. A comparison of the performance of homemade DHzFCs using self-supported HzOR catalysts.

Anode || Cathode	$c(N_2H_4)/(OH^-)$	Temp. (℃)	OCV (V)	P_{max} (mW cm^{-2})	Reference
p-Co/CF || Pt/C	1.5/6.0	25	1.1	185.9	[15]
Cu Nanostructure film || Pt/C	6.3/4.0	80	1.0	160.8	[16]
FeSA/CNT || Pt/C	1.5/1.0	80	0.83	97.1	[17]
Ni_3N-Co_3N PNAs/NF || Pt/C	0.5/1.0	25	1.0	60.3	[18]
Mo-Ni_3N/Ni/NF || Pt/C	0.5/1.0	25	0.96	37.8	[19]
FeNiP-NPHC || FeNiP-NPHC	0.5/1.0	25	0.98	31	[20]
α-Ni_xP/Ni/NF || Pt/C	3.0/1.0	25	0.94	133	This work

References

1. Y. Kuang, G. Feng, P. Li, Y. Bi, Y. Li, X. Sun, *Angew. Chem. Int. Ed.*, 2016, **55**, 693-697.
2. X. L. Wang, Y. X. Zheng, M. L. Jia, L. S. Yuan, C. Peng, W. H. Yang, *Int. J. Hydrogen Energy*, 2016, **41**, 8449-8458.
3. X. P. Wen, H. B. Dai, L. S. Wu, P. Wang, *Appl. Surf. Sci.*, 2017, **409**, 132-139.
4. J. M. Wang, X. Ma, T. T. Liu, D. N. Liu, S. Hao, G. Du, R. M. Kong, A. M. Asiri, X. P. Sun, *Mater. Today Energy*, 2017, **3**, 9-14.
5. Z. B. Feng, D. G. L, L. Wang, Q. Sun, P. Lu, P. F. Xing, M. Z. An, *J. Alloys Compd.*, 2019, **788**, 1240-1245.
6. L. S. Wu, X. P. Wen, H. Wen, H. B. Dai, P. Wang, *J. Power Sources*, 2019, **412**, 71-77.
7. H. Wen, L. Y. Gan, H. B. Dai, X. P. Wen, L. S. Wu, H. Wu, P. Wang, *Appl. Catal. B-Environ.*, 2019, **241**, 292-298.
8. Z. B. Feng, D. G. L, L. Wang, Q. Sun, P. Lu, P. F. Xing, M. Z. An, *Electrochim. Acta*, 2019, **304**, 275-281.
9. X. Lin, H. Wen, D. X. Zhang, G. X. Cao, P. Wang, *J. Mater. Chem. A*, 2020, **8**, 632-638.
10. P. P. Tang, X. Lin, H. Yin, D. X. Zhang, H. Wen, J. J. Wang, P. Wang, *ACS Sustainable Chem. Eng.*, 2020, **8**, 16583-16590.
11. P. P. Tang, H. Wen, P. Wang, *Chem. Eng. J.*, 2022, **431**, 134123.
12. Z. Y. Zhang, P. P. Tang, H. Wen, P. Wang, *J. Alloys Compd.*, 2022, **906**, 164370.
13. C. Chen, H. Wen, P. P. Tang, P. Wang, *ACS Sustainable Chem. Eng.*, 2021, **9**, 4564-4570.
14. W. T. Dai, H. Wen, Z. Y. Zhang, P. Wang, *J. Alloys Compd.*, 2022, **902**, 163746.
15. Q. Liu, X. Liao, Y. Tang, J. Wang, X. Lv, X. Pan, R. Lu, Y. Zhao, X.-Y. Yu and H. B. Wu, *Energy Environ. Sci.*, 2022, **15**, 3246-3256.
16. Z. Lu, M. Sun, T. Xu, Y. Li, W. Xu, Z. Chang, Y. Ding, X. Sun and L. Jiang, *Adv. Mater.*, 2015, **27**, 2361-2366.
17. J. Zhang, Y. Wang, C. Yang, S. Chen, Z. Li, Y. Cheng, H. Wang, Y. Xiang, S. Lu and S. Wang, *Nano Res.*, 2021, **14**, 4650-4657.

18. Q. Qian, J. Zhang, J. Li, Y. Li, X. Jin, Y. Zhu, Y. Liu, Z. Li, A. El-Harairy, C. Xiao, G. Zhang, Y. Xie, Angew. Chem. Int. Ed., 2021, 60, 5984-5993.
19. Y. Liu, J. Zhang, Y. Li, Q. Qian, Z. Li and G. Zhang, *Adv. Funct. Mater.*, 2021, **31**, 2103673.
20. Q. Yu, X. Liu, G. Liu, X. Wang, Z. Li, B. Li, Z. Wu and L. Wang, *Adv. Funct. Mater.,* 2022, **32**, 2205767.